15 November 2001

ELSEVIER

Optics Communications 199 (2001) 117–126

OPTICS COMMUNICATIONS

www.elsevier.com/locate/optcom

Power broadening revisited: theory and experiment

N.V. Vitanov [*,1], B.W. Shore [2], L. Yatsenko [3], K. Böhmer, T. Halfmann, T. Rickes, K. Bergmann

Fachbereich Physik, Universität Kaiserslautern, 67653 Kaiserslautern, Germany

Abstract

The spectral width of an atomic absorption line, observed with a steady light source, typically increases as the light intensity increases, an effect known as power broadening. In this paper, we point out classes of pulsed-light observations where power broadening does not always occur. We present analytical and numerical results, supported by experimental data of coherent pulsed excitation probed by photoionization, which show that the extent of power broadening depends crucially upon the nature of excitation and the type of measurement. In particular, we show that a spectral line obtained from measurement performed after pulsed excitation exhibits no power broadening. For pulsed excitation and continuous measurement, the spectral line contains two components: a power-broadened signal collected during the excitation and an unbroadened signal collected after the excitation. © 2001 Published by Elsevier Science B.V.

Keywords: Power broadening; Line shape; Pulsed excitation; Adiabatic evolution

1. Introduction

Observations of radiation attenuation by vapor display a well-known frequency variation of transmitted intensity—a spectral line. Such spectral line profiles are found in a variety of other observations, for example in photoionization or fluorescence from the upper state in a laser-excited two-state transition.

The width of a spectral line is affected by such factors as spontaneous emission (natural broadening), atomic motion (Doppler broadening), and vapor density (pressure broadening) [1–4]. The line profile may also be affected by the radiation intensity (power broadening) [5,6]: it is a common assumption that the line width increases as the excitation laser intensity increases. However, the present work will show theoretically, and demonstrate with experimental results, that power broadening does not always occur and that, when present, its extent depends crucially upon the nature of excitation and the type of measurement. Specifically, we will show that spectral lines obtained by coherent pulsed excitation reveal different behavior than spectral lines obtained by steady-state excitation. For coherent pulsed excitation,

* Corresponding author. Also at Helsinki Institute of Physics, University of Helsinki, PL 9, 00014 Helsinki, Finland.

E-mail address: vitanov@rock.helsinki.fi (N.V. Vitanov).

[1] Permanent address: Department of Physics, Sofia University, James Boucher 5 Boulevard, 1126 Sofia, Bulgaria; also at Institute of Solid State Physics, Bulgarian Academy of Sciences, Tsarigradsko shaussée 72, 1784 Sofia, Bulgaria.

[2] Permanent address: Lawrence Livermore National Laboratory, Livermore, CA 94550, USA.

[3] Permanent address: Institute of Physics, Ukrainian Academy of Sciences, prospect Nauki 46, 252650 Kiev-22, Ukraine.

0030-4018/01/$ - see front matter © 2001 Published by Elsevier Science B.V.
PII: S0030-4018(01)01495-X

measurement performed after the excitation produces spectral lines with different properties compared to measurement performed during the excitation. Thus the present paper develops and extends earlier studies of spectral lines in pulsed excitation [7,8].

In the remainder of this introductory section, we define various signals for different types of excitation and observation. Section 2 presents a general theoretical description of coherent two-state pulsed excitation with loss. In Section 3, we describe an exactly solvable analytic model that allows explicit evaluation of two contributions to the line profile, only one of which exhibits power broadening. Section 4 presents experimental data supporting these theoretical results. Section 5 gives a summary of the results.

1.1. Steady-state excitation, continuous measurement

The simplest and most traditional spectral lines are observed in a steady-state situation, when atomic populations acquire values determined by an equilibrium between cw radiative excitation and various relaxation processes, such as spontaneous emission and collisional relaxation. Then the experimentally measured signal S_{steady} (resulting, for example, from absorption, fluorescence, or photoionization) is proportional to the steady-state population in the excited state $\langle P_2 \rangle$. The dependence of the signal on the detuning $\Delta = \omega_0 - \omega$, the difference between the atomic Bohr frequency ω_0 and the laser frequency ω, defines the spectral line. As discussed in standard texts (e.g. Ref. [6], p. 219), for an ensemble of identical two-state atoms the spectral line has a Lorentzian dependence on Δ,

$$S_{\text{steady}} \propto \langle P_2 \rangle = \frac{1}{2} \frac{(I/I_{\text{sat}})}{1 + (\Delta/\beta)^2 + (I/I_{\text{sat}})}, \tag{1}$$

where the saturation intensity I_{sat} is a characteristic parameter of the particular transition, and β is the width parameter in the weak-excitation limit (a combination of spontaneous emission and any relaxation processes). Eq. (1) presents a conventional view of power broadening: an increase of radiation intensity I is expected to increase the width of some Lorentzian line profile.

Such power broadening occurs because, as the excitation field becomes more intense, the atoms spend a greater fraction of time in the excited state, though never more than the saturation value of 1/2. The line width is proportional to the range of detunings where saturation occurs. Because this range increases with the laser intensity, such observations exhibit power broadening.

1.2. Pulsed coherent excitation and delayed measurement

Pulsed excitation can differ significantly from steady-state excitation if the pulse is much shorter than the relaxation times. Coherence is then important, and rate-equation analysis is invalid. Suppose, for example, that the signal S_{pulsed} is produced by a photoionizing probe field which is applied after the excitation pulse, but before the excited state can decay radiatively, and which ionizes only the excited atoms. Then the ionization signal S_{pulsed} is proportional to the population of the excited state $P_2(t_{\text{f}})$ at the cessation time of the pulse t_{f}. Hence for exactly resonant excitation ($\Delta = 0$),

$$S_{\text{pulsed}} \propto P_2(t_{\text{f}}) = \sin^2(A/2), \tag{2}$$

where the pulse area A is the time integrated Rabi frequency, $A = \int_{t_{\text{i}}}^{t_{\text{f}}} \Omega(t)\,\mathrm{d}t$. The Rabi frequency $\Omega(t)$ quantifies the coherent laser–atom interaction [9]. For an electric-dipole single-photon transition, $\Omega(t)$ is proportional to the laser electric-field amplitude. For a two-photon transition, $\Omega(t)$ is proportional to the square of the laser electric field, i.e. to the laser intensity.

When there is some variation of pulse areas amongst the atoms, e.g. due to spatial inhomogenities or different velocities, then observations will measure an average over areas. For resonant excitation this averaging places half of the population into the excited state.

If the laser carrier frequency is detuned from resonance, the amplitude of the population oscillations decreases, and so does the average excited-state population. One might argue that, if the Rabi

frequency is significantly larger than the detuning, then the excitation will differ little from that of exact resonance (saturation), and that after an average over pulse areas, again half of the population will be excited at the end of the pulse. Then one would also expect that, as for steady-state excitation, the saturation intensity will grow with the detuning and therefore the signal will experience power broadening. However, as we will show in this work, for coherent excitation this conclusion is wrong.

The key point is that a smooth laser pulse, irrespective of its intensity, produces an appreciable excitation only for detunings $|\Delta| \lesssim 1/T$, where T is the pulse duration (Section 2.2). For detunings $|\Delta| \gtrsim 1/T$ the evolution is adiabatic; then the population, after a possible excursion to the excited state during the action of the excitation pulse, returns to the initial state at the end of the pulse, i.e. there is, for any laser intensity, complete population return [8,10,11]. For detunings in the range $|\Delta| \lesssim 1/T$ the evolution is not adiabatic, and so appreciable population can remain in the excited state after the excitation pulse; this range determines the line width. Because this detuning range does not depend on the laser intensity, measurements performed after pulsed excitation will exhibit no power broadening: for any laser intensity the line width is $1/T$, apart from a numerical factor depending on the pulse shape.

1.3. Pulsed coherent excitation and steady measurement

Alternatively, we can consider a photoionization signal produced by a steady probe field (or, equivalently, a continuously detected fluorescence signal) and a pulsed coherent excitation field. During the presence of the excitation pulse the probe samples the average transient excitation (power broadened), whereas after the excitation pulse there occurs a further signal (not broadened). Thus one will observe a combination of a narrow feature with the width $1/T$, immune to power broadening, and a power-broadened feature with width determined by the excitation Rabi frequency. This most general situation is the subject of the present paper.

2. Theoretical model

To quantify these considerations, we examine a simple idealized model: a two-state system, coherently excited by a laser pulse, whose excited-state population is measured by a photoionizing probe laser. We model photoionization by introducing a loss rate Γ from the excited state ψ_2: continuous measurement is described by constant Γ, and (delayed) pulsed measurement by pulse-shaped time-dependent Γ. We assume that there are no other relaxation processes, and so the dynamics is governed by the time-dependent Schrödinger equation,

$$\mathrm{i}\hbar \frac{\mathrm{d}}{\mathrm{d}t}\mathbf{C}(t) = \mathsf{H}(t)\mathbf{C}(t), \tag{3}$$

where $\mathbf{C}(t) = [C_1(t), C_2(t)]^{\mathrm{T}}$ is a column vector formed by the probability amplitudes of the two states. The Hamiltonian describing this system is given in the rotating-wave approximation by [9]

$$\mathsf{H}(t) = \hbar \begin{bmatrix} 0 & \frac{1}{2}\Omega(t) \\ \frac{1}{2}\Omega(t) & \Delta - \frac{1}{2}\mathrm{i}\Gamma \end{bmatrix}, \tag{4}$$

in which the time-dependent Rabi frequency $\Omega(t)$ couples the ground state ψ_1 with the excited state ψ_2, and Δ is the atom–laser detuning. The system is taken to be initially in its ground state, $C_1(t_\mathrm{i}) = 1$, $C_2(t_\mathrm{i}) = 0$, and the populations of the two states at the final time of the interaction t_f are $P_k(t_\mathrm{f}) = |C_k(t_\mathrm{f})|^2$, $(k = 1, 2)$.

It proves appropriate to define the signal as $S = 1 - P_1(t_\mathrm{f})$. If the measurement is performed after the excitation (so that there are no losses during the excitation, $\Gamma = 0$), then S is the measured excited-state population $S = P_2(t_\mathrm{f})$ produced by the excitation pulse. For continuous measurement, performed during and after the excitation (when the loss rate is nonzero, $\Gamma > 0$), S expresses the population lost from the two-state system, which again is the measured signal.

2.1. The adiabatic basis

In order to understand power broadening for coherent pulsed excitation, it is convenient to introduce the adiabatic states—the instantaneous eigenstates of the real part of the Hamiltonian (4),

$$\Phi_-(t) = \psi_1 \cos\vartheta(t) - \psi_2 \sin\vartheta(t), \tag{5}$$

$$\Phi_+(t) = \psi_1 \sin\vartheta(t) + \psi_2 \cos\vartheta(t), \tag{6}$$

where

$$\vartheta(t) = \frac{1}{2}\arctan\frac{\Omega(t)}{\Delta}, \tag{7}$$

and the bare states ψ_1 and ψ_2 each include an implicit time-dependent phase originating with the rotating wave transformation. The adiabatic states satisfy the relation $\mathsf{H}(\Gamma = 0)\Phi_\pm = \hbar\lambda_\pm\Phi_\pm$, with eigenvalues

$$\lambda_\pm(t) = \frac{1}{2}\left[\Delta \pm \sqrt{\Omega^2(t) + \Delta^2}\right]. \tag{8}$$

The probability amplitudes of the bare states $\mathbf{C}(t) = [C_1(t), C_2(t)]^{\mathrm{T}}$ and the adiabatic states $\mathbf{B}(t) = [B_-(t), B_+(t)]^{\mathrm{T}}$ are connected via the orthogonal transformation $\mathbf{C}(t) = \mathsf{R}[\vartheta(t)]\mathbf{B}(t)$, where

$$\mathsf{R}(\vartheta) = \begin{bmatrix} \cos\vartheta & \sin\vartheta \\ -\sin\vartheta & \cos\vartheta \end{bmatrix}. \tag{9}$$

The Schrödinger equation in the adiabatic basis reads

$$\mathrm{i}\hbar\frac{\mathrm{d}}{\mathrm{d}t}\mathbf{B}(t) = \mathsf{H}_b(t)\mathbf{B}(t), \tag{10}$$

with

$$\begin{aligned}\mathsf{H}_b &= \mathsf{R}(-\vartheta)\mathsf{H}\mathsf{R}(\vartheta) - \mathrm{i}\hbar\mathsf{R}(-\vartheta)\frac{\mathrm{d}}{\mathrm{d}t}\mathsf{R}(\vartheta) \\ &= \hbar\begin{bmatrix} \lambda_- - \frac{1}{2}\mathrm{i}\Gamma\sin^2\vartheta & -\mathrm{i}\dot{\vartheta} - \frac{1}{4}\mathrm{i}\Gamma\sin 2\vartheta \\ \mathrm{i}\dot{\vartheta} - \frac{1}{4}\mathrm{i}\Gamma\sin 2\vartheta & \lambda_+ - \frac{1}{2}\mathrm{i}\Gamma\cos^2\vartheta \end{bmatrix}.\end{aligned} \tag{11}$$

We assume that the pulsed Rabi frequency $\Omega(t)$ is negligible outside the finite time interval $t_\mathrm{i} < t < t_\mathrm{f}$. Because the detuning Δ is assumed constant, we have $\vartheta(t_\mathrm{i}) = \vartheta(t_\mathrm{f}) = 0$. Therefore before and after the excitation each adiabatic state (11) becomes uniquely identified with the same bare state,

$$\begin{aligned}\Phi_-(t_\mathrm{i}) &= \Phi_-(t_\mathrm{f}) = \psi_1, \\ \Phi_+(t_\mathrm{i}) &= \Phi_+(t_\mathrm{f}) = \psi_2.\end{aligned} \tag{12}$$

Eq. (12) show that if the evolution is adiabatic—and hence the population remains in the same adiabatic state in which it starts, i.e., in $\Phi_-(t)$—the population will always return to the initial state ψ_1 at the end of the excitation, irrespective of the specific Rabi frequency. We will show below that, for exponentially vanishing pulses, the evolution is not adiabatic only inside a detuning range of the order of the inverse pulse width T^{-1}.

2.2. The adiabatic condition

As follows from Eq. (11), the condition for adiabatic evolution for $\Gamma = 0$ is $|\dot{\vartheta}(t)| \ll \lambda_+(t) - \lambda_-(t)$ or, explicitly,

$$|\Delta\,\dot{\Omega}(t)| \ll 2[\Omega^2(t) + \Delta^2]^{3/2}.$$

It is convenient to define the function

$$f(t) = \frac{\Delta\,\dot{\Omega}(t)}{2[\Omega^2(t) + \Delta^2]^{3/2}}; \tag{13}$$

the adiabatic condition (13) then reads $|f(t)| \ll 1$. It is easily seen that $|f(t)|$, considered as a function of Δ, has maxima at $\Delta = \pm(1/\sqrt{2})\Omega(t)$; its maximum value is

$$|f(t)|_{\max} = \frac{|\dot{\Omega}(t)|}{3\sqrt{3}\Omega^2(t)}.$$

Let us assume that the peak value Ω_0 of the Rabi frequency $\Omega(t)$ occurs at time $t = 0$. Obviously, near $t = 0$, $|f(t)|_{\max}$ has its smallest values, because $\Omega(t)$ has its maximum there, $\Omega(0) = \Omega_0$, and $|\dot{\Omega}(t)|$ has its minimum, $|\dot{\Omega}(0)| = 0$. Hence, nonadiabatic transitions are more likely to occur at early and late times. At large times, the derivative of a function vanishing exponentially, such as hyperbolic secant $\Omega(t) = \Omega_0\,\mathrm{sech}(t/T)$, is proportional to the function itself, i.e., $|\dot{\Omega}(t)| \approx \Omega(t)/T$. For such functions, we find that

$$|f(t)|_{\max} \approx \frac{1}{3\sqrt{6}|\Delta|T}.$$

Hence for adiabatic evolution, the product of the detuning and the pulse width must exceed unity,

$$|\Delta|T \gtrsim 1. \tag{14}$$

This inequality defines the adiabatic region for an exponentially vanishing pulse: the evolution is adiabatic for $|\Delta T| \gtrsim 1$ and nonadiabatic for $|\Delta T| \lesssim 1$.

The important observation from the adiabatic condition (14) is that it does not depend on the peak Rabi frequency Ω_0.

We point out that other, nonexponential pulse shapes, e.g. Gaussian, may lead to a slight dependence of the line width on the Rabi frequency. However, for smooth pulse shapes, such dependences are very weak.

2.3. Line width of a signal measured after excitation

In the adiabatic limit, the nonadiabatic coupling $\dot{\vartheta}(t)$ is, by definition, negligibly small compared to the eigenvalue splitting, and it can be neglected. In the absence of losses ($\Gamma = 0$) the adiabatic solution for the bare-state populations reads

$$P_1(t) = \cos^2\vartheta(t) = \frac{1}{2} + \frac{\Delta}{2\sqrt{\Omega^2(t) + \Delta^2}}, \tag{15}$$

$$P_2(t) = \sin^2\vartheta(t) = \frac{1}{2} - \frac{\Delta}{2\sqrt{\Omega^2(t) + \Delta^2}}. \tag{16}$$

Because $\Omega(t_f)$ is negligibly small, the excited-state population at the end of the excitation is negligible, $P_2(t_f) \approx 0$. Therefore outside the nonadiabaticity region, no excitation will remain at the end of the pulse. Hence the line width of a signal measured after the excitation cannot be larger than the nonadiabatic region around $\Delta = 0$. According to Eq. (14), this region is bounded by $|\Delta| \lesssim 1/T$, and so it does not depend on the peak Rabi frequency Ω_0. Thus, if we plot $P_2(t_f)$ against Δ, we will observe no power broadening.

2.4. Line width of a signal measured during excitation

When the signal is collected during the excitation, it is the transient excitation picture that matters, rather than the final populations, because the signal is proportional to the average transient excited-state population. Moreover, because for any detuning, the transient excited-state population increases with the laser intensity, there is no qualitative difference between diabatic and adiabatic evolution. Indeed, as Eq. (16) shows, during adiabatic excitation the population $P_2(t)$ can reach significant values—the larger the Rabi frequency, the larger the population $P_2(t)$. Because $P_2(t)$ scales with the ratio Δ/Ω_0, a signal measured during the excitation will exhibit power broadening.

We can obtain a simple estimate of a continuously detected signal in the case of weak losses ($\Gamma/4 \ll \lambda_+ - \lambda_-$) and adiabatic evolution. Then we can neglect, along with $\dot{\vartheta}(t)$, the Γ-terms in the off-diagonal elements of Eq. (11); then the losses come mainly from the diagonal elements. From the resulting diagonal Hamiltonian, we obtain

$$P_1(t) = \exp\left[-\Gamma\int_{t_i}^{t}\sin^2\vartheta(t')\,dt'\right]\cos^2\vartheta(t), \tag{17}$$

$$P_2(t) = \exp\left[-\Gamma\int_{t_i}^{t}\sin^2\vartheta(t')\,dt'\right]\sin^2\vartheta(t). \tag{18}$$

The ionization signal at the end of the interaction is

$$S = 1 - P_1(t_f) = 1 - \exp\left[-\Gamma\int_{t_i}^{t_f}\sin^2\vartheta(t')\,dt'\right].$$

Since S depends on Ω_0 and Δ only via ϑ, which in turn depends only on the ratio Ω_0/Δ, the signal S must scale with Ω_0/Δ. Hence the signal experiences power broadening: its FWHM $\Delta_{1/2}$ is proportional to Ω_0.

3. Analytic model

3.1. The model

An illustration of the preceding theory is provided by an analytically solvable model which assumes a hyperbolic-secant pulse, constant detuning, and constant loss rate,

$$\Omega(t) = \Omega_0\,\mathrm{sech}(t/T), \tag{19}$$

$$\Delta = \mathrm{const}, \tag{20}$$

$$\Gamma = \mathrm{const}. \tag{21}$$

This model is a particular case of the lossy Demkov–Kunike model [12], where the detuning contains an additional hyperbolic-tangent term.

The present model in turn reduces to the lossless Rosen–Zener model [13] for $\Gamma = 0$.

3.2. The solution

The ionization signal for this model can be derived analytically. It is given by [12]

$$S = 1 - \left| \frac{\Gamma^2(\frac{1}{2} + \gamma + \mathrm{i}\delta)}{\Gamma(\frac{1}{2} + \alpha + \gamma + \mathrm{i}\delta)\Gamma(\frac{1}{2} - \alpha + \gamma + \mathrm{i}\delta)} \right|^2, \tag{22}$$

where $\Gamma(z)$ is the Euler's gamma function (not to be confused with the loss rate!), and we have introduced the dimensionless parameters

$$\alpha = \frac{\Omega_0 T}{2}, \quad \delta = \frac{\Delta T}{2}, \quad \gamma = \frac{\Gamma T}{4}.$$

By using the reflection formula $\Gamma(z)\Gamma(1-z) = \pi/\sin(\pi z)$, we can rewrite Eq. (22) in the equivalent form

$$S = S^{(1)} + S^{(2)}, \tag{23}$$

where

$$S^{(1)} = \frac{\sin^2 \pi(\alpha - \gamma)}{\cosh^2 \pi\delta}, \tag{24}$$

$$S^{(2)} = (1 - S^{(1)}) \left[1 - \left| \frac{\Gamma(\frac{1}{2} + \gamma + \mathrm{i}\delta)}{\Gamma(\frac{1}{2} + \mathrm{i}\delta)} \right|^4 \times \left| \frac{\Gamma(\frac{1}{2} + \alpha - \gamma + \mathrm{i}\delta)}{\Gamma(\frac{1}{2} + \alpha + \gamma + \mathrm{i}\delta)} \right|^2 \right]. \tag{25}$$

In the absence of losses during the excitation ($\Gamma = 0$), $S^{(2)} = 0$ and Eq. (23) reduces to the Rosen–Zener formula [13]

$$S = S^{(1)} = \frac{\sin^2(\frac{1}{2}\pi\Omega_0 T)}{\cosh^2(\frac{1}{2}\pi\Delta T)}, \quad (\Gamma = 0). \tag{26}$$

Then the FWHM of the line profile $S(\Delta)$,

$$\Delta_{1/2} = \frac{4}{\pi T} \ln(1 + \sqrt{2}), \quad (\Gamma = 0), \tag{27}$$

is solely determined by the pulse duration T and does not depend on the Rabi frequency Ω_0 at all; hence for lossless excitation, there is no power broadening for the hyperbolic-secant pulse.

In the presence of losses during the excitation ($\Gamma \neq 0$), we can approximate Eq. (25) by using the formula

$$\ln \frac{\Gamma(z+\gamma)}{\Gamma(z)} \approx \gamma \ln z - \gamma + \mathcal{O}(z^{-1}), \tag{28}$$

which derives from the Stirling formula [14],

$$\ln \Gamma(z) \approx \left(z - \tfrac{1}{2}\right) \ln z - z + \tfrac{1}{2} \ln 2\pi + \mathcal{O}(z^{-1}).$$

The approximate formula for $S^{(2)}$, valid for $\alpha, \delta \gg 1$, is given by

$$S^{(2)} \approx (1 - S^{(1)}) \left[1 - \left(\frac{\delta^2}{\alpha^2 + \delta^2} \right)^{2\gamma} \right]. \tag{29}$$

For smaller α and δ, a good approximation can be obtained from Eq. (25) by using first the identity $z\Gamma(z) = \Gamma(z+1)$ (possibly repeatedly), and then formula (28).

3.3. Discussion

There is a significant qualitative difference between the two terms $S^{(1)}$ and $S^{(2)}$ of the signal (23) in their dependences on the loss rate Γ: the term $S^{(2)}$ depends very strongly on Γ, while in $S^{(1)}$, Γ only causes a shift in the oscillation phase. Furthermore, the term $S^{(2)}$ vanishes in the limit $\Gamma = 0$, while the term $S^{(1)}$ survives; hence, the term $S^{(1)}$ results from decay after the excitation, while the term $S^{(2)}$ comes from decay during the action of the excitation pulse.

The two terms $S^{(1)}$ and $S^{(2)}$ differ considerably also in their dependences on the detuning Δ. The term $S^{(1)}$ shows no power broadening at all and its FWHM $\Delta^{(1)}_{1/2}$ is given by Eq. (27). In contrast, the FWHM $\Delta^{(2)}_{1/2}$ of $S^{(2)}$ shows typical power broadening: indeed, as Eq. (29) shows, the square-bracket term of $S^{(2)}$ depends on Δ and Ω_0 only via the ratio $\alpha/\delta = \Omega_0/\Delta$ and therefore, its width $\Delta^{(2)}_{1/2}$ is proportional to the peak Rabi frequency Ω_0.

In conclusion, the total ionization signal (23) in the lossy Demkov–Kunicke model (12) is a sum of a term $S^{(1)}$, which results from decay after the excitation and therefore exhibits no power broadening, and a power-broadened term $S^{(2)}$, which results from decay during the action of the excitation pulse. The width of the term $S^{(1)}$ is

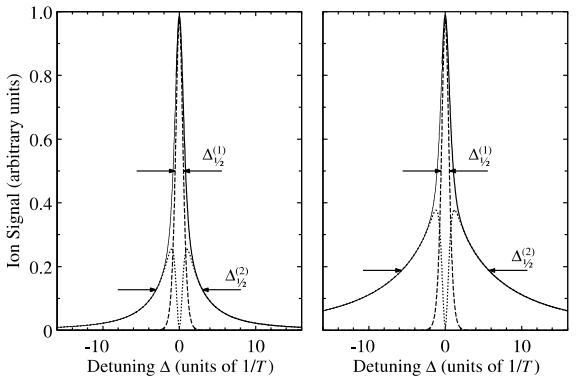

Fig. 1. Ionization signal S for the hyperbolic-secant pulse, plotted against the detuning Δ for loss rate $\Gamma = 0.2T^{-1}$ and two peak Rabi frequencies, $\Omega_0 = 5T^{-1}$ (left frame) and $\Omega_0 = 15T^{-1}$ (right frame). The solid curve shows the exact result (23), the long-line dashed curve shows the term $S^{(1)}$ (24), and the short-line dashed curve shows the term $S^{(2)}$ (25). The term $S^{(1)}$ dominates around the resonance, while $S^{(2)}$ dominates at large detuning. The line width $\Delta^{(1)}_{1/2}$ of $S^{(1)}$ does not depend on Ω_0, while the line width $\Delta^{(2)}_{1/2}$ of $S^{(2)}$ increases with Ω_0, indicating power broadening.

proportional to the inverse pulse width, $\Delta^{(1)}_{1/2} \propto 1/T$, while the width of the term $S^{(2)}$ is proportional to the peak Rabi frequency, $\Delta^{(2)}_{1/2} \propto \Omega_0$. Hence, for large Rabi frequencies ($\Omega_0 T \gg 1$), the term $S^{(1)}$ dominates for small detuning ($|\Delta|T \lesssim 1$), while the term $S^{(2)}$ dominates for large detuning ($|\Delta|T \gtrsim 1$).

In Fig. 1, the signal (23) is plotted versus the detuning Δ for two different peak Rabi frequencies, $\Omega_0 = 5T^{-1}$ and $15T^{-1}$. The figure demonstrates that, while the width $\Delta^{(1)}_{1/2}$ of the $S^{(1)}$ term does not depend on the Rabi frequency, the $S^{(2)}$ term shows typical power broadening.

4. Experiment

Our experiments were designed to reveal the two components of a line profile, only one of which exhibits power broadening. The experiment proceeded through two steps. In the first step, an excitation pulse produced an excited state. In the second step, a delayed probe pulse produced photoionization from the excited state. The line profile of interest was a plot of ionization signal versus detuning of the excitation carrier frequency from resonance. The extent to which the profile was power broadened was adjustable by varying the delay, and therefore the overlap, between the excitation and probe pulses.

4.1. Description of experiment

We performed the experiments on a pulsed beam of metastable helium atoms, prepared with apparatus described in detail elsewhere [15,16]. The excitation pulse excited atoms from the metastable state 2^3S_1 to the excited state 3^3S_1 by means of a two-photon transition; a probe field ionized these excited atoms. The excitation pulse, with a duration of 4.9 ns (FWHM), was produced by amplifying 855 nm radiation from a cw single-mode Ti:sapphire ring laser in a pulsed dye amplifier. The dye was pumped by the second harmonic, at 532 nm wavelength, of an injection seeded Nd:YAG laser (Quanta-Ray GCR 4). A portion of the second harmonic was used as the probe pulse, photoionizing the 3^3S_1 state, with a pulse duration of 6.2 ns (FWHM). The ions passed through a 30 cm time-of-flight segment, and were detected mass selectively with a double-thickness microsphere plate (El Mul Technologies). The output current of the microsphere plate was amplified with fast broadband amplifiers and integrated in a boxcar-gated integrator (EG&G) to provide the signal for display as a line profile.

The temporal profiles of the excitation and probe pulses were very close to Gaussian, with pulse energies up to 5.5 mJ for the excitation and 30 mJ for the probe. An optical delay line provided adjustable offsets in time. The two beams were slightly focused and spatially overlapped in the interaction region, where the beam diameters were about 0.3 mm for the excitation beam and 0.5 mm for the probe beam. This arrangement provided intensities up to 2 GW/cm^2 for each beam.

4.2. Numerical simulation

To supplement the experimental results presented below, we carried out numerical simulation of the ionization profile by integrating the Schrödinger equation. These results are shown as

solid lines in the following figures. In the simulations, we used atomic parameters calculated in Ref. [17] using the model potential method described in Ref. [15]. The effective Stark shift was taken as $S = S^{(1)} - S^{(2)} = 23I_p$ and the two-photon ionization rate of state $3\,^3S_1$ by the excitation laser was calculated as $\Gamma = 0.1 \times 10^{-9} I_p$, where S and Γ are expressed in s^{-1} and I_p in W/cm^2. Our computations took into account intensity fluctuations of the excitation laser and integration over both lasers spatial profiles.

4.3. Results for long delay

We first consider cases when there is a long delay, 11 ns, between the excitation pulse and the ionizing probe pulse, so that the ionization measurement is performed after the excitation is completed, but before the excited-state population is affected significantly by spontaneous emission (the lifetime of the $3\,^3S_1$ state is 36 ns). Fig. 2 shows the measured ionization signal from state $3\,^3S_1$ of helium versus the excitation laser detuning for two maximum intensities, 37 and 120 MW/cm^2, when the ionizing probe pulse is applied 11 ns after the excitation pulse.

The line profile here is dominated by a narrow central feature that exhibits little power broadening when the excitation intensity increases by more than a factor of three. Underlying this narrow feature is a broader feature, seen at the higher power. This power-broadened part is due to two-photon ionization of the $3\,^3S_1$ state by the excitation laser during the excitation. That is, the excitation supplements the probe in producing ionization. This power broadened contribution is what we would expect from the discussion above. The slight asymmetry of the lines is caused by the Stark shifts. In both cases there is a very good agreement between the experimental data (dots) and the numerical simulations (solid line).

4.4. Results for short delay

We next consider cases in which there is only a short delay between excitation and probe, so there is some overlap of the excitation and ionization pulses. Fig. 3 shows the ionization signal for two intensities, 75 and 300 MW/cm^2, when the delay is 4.7 ns.

The line shape here differs noticeably from Lorentzian form. It can be considered as a superposition of contributions from different probe times. For early times (when the excitation and probe pulses overlap) this contribution is power broadened. For late times (when the excitation pulse has vanished) there is no power broadening. The width of the profile increases with increasing excitation intensity but it is not directly proportional to that intensity. In Fig. 3, the maximum

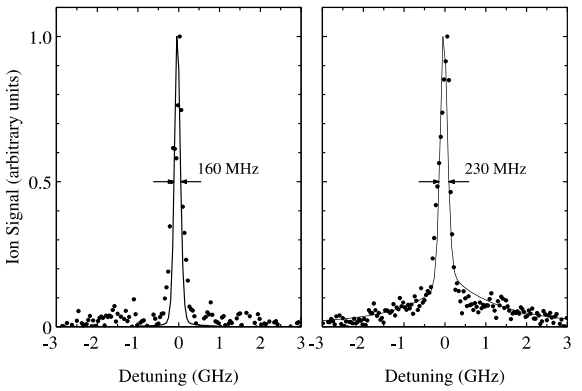

Fig. 2. Ionization signal versus excitation laser detuning for a (long) delay of 11 ns between excitation and probe pulses for excitation laser intensities of 37 MW/cm^2 (left frame) and 120 MW/cm^2 (right frame). Dots show experimental results and solid lines show numerical simulation values.

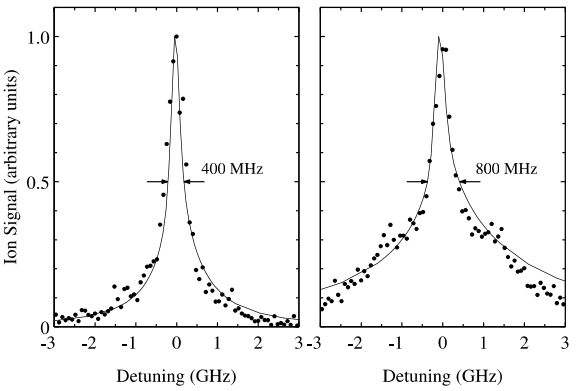

Fig. 3. Ionization signal versus excitation laser detuning for a (short) delay of 4.7 ns between excitation and probe pulses for excitation laser intensities of 75 MW/cm^2 (left frame) and 300 MW/cm^2 (right frame). Dots show experimental results and solid lines show numerical simulation values.

intensity is increased by a factor of four but the line width is only doubled. This result confirms our prediction that for partially overlapping excitation and probe pulses the line profile shows more significant power broadening than for separated excitation and probe pulses. As with the long-delay cases, the numerical simulation fits the experimental results quite well.

It is particularly instructive to compare Fig. 2 (right frame) with Fig. 3 (left frame). Although the laser intensity of 120 MW/cm^2 in Fig. 2 (right frame) is considerably larger than the 75 MW/cm^2 intensity in Fig. 3 (left frame), the line width in the former case is much smaller: 230 MHz compared to 400 MHz. The reason is that in the former case the measurement is performed after the excitation, while in the latter case the measurement is performed partly during the excitation. This is a clear demonstration of the importance of the type of measurement for the extent of power broadening of the line profile.

5. Conclusions

The present paper has shown that a common notion in coherent atomic excitation—power broadening—does not always occur, and its presence depends critically on the nature of excitation and the type of measurement.

Typical power broadening, with a Lorentzian profile, is observed when one monitors continuosly, for example by photoionization or fluorescence, the excited-state population in a two-state system driven by a cw laser field. Then for any detuning, an increase of laser intensity causes more population to visit the excited state, and so increases the signal. The line width is determined by the range of detunings for which the excited state acquires appreciable transient population during the excitation pulse; because this detuning range increases with the excitation intensity, such observations display power broadening.

However, power broadening cannot be taken for granted in the case of pulsed excitation. When the measurement is separated from the excitation stage, so that the signal measures the excited-state population after the excitation, power broadening does not occur. The reason is that for a lossless pulsed excitation, appreciable excited-state population remains at the end of the pulse only for detunings $|\Delta| \lesssim 1/T$, because in this range the evolution is not adiabatic. For detunings $|\Delta| \gtrsim 1/T$, the excitation pulse produces adiabatic evolution and the population, after making an excursion to the excited state during the action of the pulse, returns to the ground state at the end of the pulse. Because the nonadiabatic detuning range does not depend (or depends very slightly) on the laser intensity, but only on the pulse width T, there is little or no power broadening.

Our experiments, which used a time-delayed ionizing probe pulse, illustrated examples of these points. In particular, the experiments displayed considerable reduction of power broadening when the probe pulse delay increased, so that the measurement could be separated from the excitation stage.

Acknowledgements

This work has received partial support from the European Community's Human Potential Programme under contract HPRN-CT-1999-00129. NATO grant 1507-826991, Deutsche Forschungsgemeinschaft, and INTAS project 99-00019. NVV has received partial support from the Academy of Finland, project 43336. BWS acknowledges the support of Laserzentrum, University of Kaiserslautern, and the Alexander von Humboldt Stiftung for a Research Award.

References

[1] R.G. Breene, The Shift and Shape of Spectral Lines, Pergamon, NY, 1961.
[2] R.G. Breene, Theories of Spectral Line Shapes, Wiley, NY, 1981.
[3] H.R. Griem, Plasma Spectroscopy, McGraw-Hill, NY, 1964.
[4] I.I. Sobel'man, L.A. Vainshtein, E.A. Yukov, Excitation of Atoms and Broadening of Spectral Lines, Springer, NY, 1981.
[5] L. Allen, J.H. Eberly, Optical Resonance and Two Level Atoms, Dover, NY, 1975.
[6] P.W. Milonni, J.H. Eberly, Lasers, Wiley, NY, 1988.
[7] N. Essarroukh, J. Jureta, P.C. Karangwa, X. Urbain, F. Brouillarg, Proceedings of XX ICPEAC, vol. II, 1997, p. TU040.

[8] A. Kuhn, S. Steuerwald, K. Bergmann, Eur. Phys. J. D 1 (1998) 57.
[9] B.W. Shore, The Theory of Coherent Atomic Excitation, Wiley, NY, 1990.
[10] N.V. Vitanov, J. Phys. B 28 (1995) L19.
[11] N.V. Vitanov, P.L. Knight, J. Phys. B 28 (1995) 1905.
[12] N.V. Vitanov, S. Stenholm, Phys. Rev. A 55 (1998) 2983.
[13] N. Rosen, C. Zener, Phys. Rev. 40 (1932) 502.
[14] M. Abramowitz, I.A. Stegun (Eds.), Handbook of Mathematical Functions, Dover, New York, 1964.
[15] L.P. Yatsenko, T. Halfmann, B.W. Shore, K. Bergmann, Phys. Rev. A 59 (1999) 2926.
[16] T. Halfmann, J. Koensgen, K. Bergmann, Meas. Sci. Technol. 11 (2000) 1510.
[17] L.P. Yatsenko, S. Guérin, T. Halfmann, K. Böhmer, B.W. Shore, K. Bergmann, Phys. Rev. A 58 (1998) 4683.